Semiconductor Laser Sources for Externally Modulated Microwave Analog Links

Gary E. Betts, *Member, IEEE,* J. P. Donnelly, *Fellow, IEEE,* J. N. Walpole, *Fellow, IEEE,* S. H. Groves, F. J. O'Donnell, L. J. Missaggia, R. J. Bailey, and A. Napoleone

***Abstract*— High-performance semiconductor continous-wave (CW) sources are demonstrated in this paper, which include a Fabry–Perot (FP) laser oscillator (LO) with relative intensity noise (RIN) < -165 dB/Hz at frequencies above 500 MHz, and a tapered semiconductor optical amplifier with 35-dB gain, a maximum output power of 820 mW, and RIN ≈ -155 dB/Hz at microwave frequencies. These are used in suboctave-bandwidth analog links to demonstrate link performance comparable to that available with solid-state laser sources.**

***Index Terms*—Laser noise, optical analog links, optical modulation, semiconductor lasers, semiconductor optical amplifiers.**

I. Introduction

SEMICONDUCTOR laser oscillators (LO's) and amplifiers have some important advantages as continuous-wave (CW) sources for externally modulated optical analog links, as compared to the traditional solid-state lasers normally used. Semiconductor laser devices directly convert dc electrical power to light at the desired wavelength, providing much higher *wall-plug* efficiency than systems such as diode-pumped solid-state lasers (DPSSL's) or erbium-doped fiber amplifiers (EDFA's), which use one or two optical-to-optical conversions after the initial electrical-to-optical conversion. Diode laser devices are also physically small compared to the alternatives. These advantages are critical in space-based systems [1], and important for links on aircraft or other platforms where power and space are limited. Since they are much simpler, the semiconductor laser devices should ultimately be less costly than DPSSL's and EDFA's. Another advantage of semiconductor lasers is their ability to operate at any wavelength in the fiber communication bands, enabling wavelength multiplexed systems and systems requiring incoherent combining of several light beams (as in several optically controlled phased-array radar schemes [2]).

There are some disadvantages to semiconductor laser devices as well. They traditionally have had low optical-power output and high relative-intensity noise (RIN) compared to DPSSL's or EDFA's, and their larger linewidth has caused interferometric intensity noise (IIN) [3] extending above 100 MHz. The primary purpose of this paper is to show that these disadvantages have been substantially overcome—at least for a large range of practical applications.

Manuscript received December 2, 1996; revised April 25, 1997. This work was supported by the U.S. Department of Air Force under AF Contract F19628-95-C-0002.

The authors are with Lincoln Laboratory, Massachusetts Institute of Technology, Lexington, MA 02173-9108 USA.

Publisher Item Identifier S 0018-9480(97)06002-X.

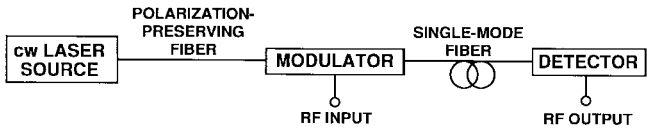

Fig. 1. Externally modulated link with CW laser source. The laser source may be a semiconductor or Nd:YAG oscillator, with or without the tapered semiconductor optical amplifier.

Several new devices and techniques will be combined here to achieve good analog-link results. Perhaps the most dramatic is the tapered semiconductor amplifier, which provides over 800-mW output at 1320 nm, overcoming the power limitations of single-mode semiconductor devices in the 1300-nm fiber transmission band. We also show results from a Fabry–Perot (FP) semiconductor LO with RIN below -165 dB/Hz at all microwave frequencies. Commercial distributed-feedback (DFB) laser diodes are available with comparable low RIN below 1 GHz, but they generally have a RIN peak above -150 dB/Hz somewhere between 5–15 GHz. We will also show how, for suboctave systems, certain modulator techniques such as suppressed-carrier bias and linearization can overcome the remaining RIN problems of semiconductor lasers. The work reported here has all been in the 1300-nm band, but it could also be done at 1550 nm.

We will first report measurements of the semiconductor laser devices themselves, and then go on to design issues and measurement of the analog links that use these devices. It should also be noted that although there are many possible ways to use the semiconductor laser devices, such as direct modulation of the oscillator or placement of the amplifier after the modulator, the only use discussed here will be as a CW source, as shown in Fig. 1.

II. FP Diode LO

We fabricated a low-noise FP diode LO to serve as an analog-link CW source. The device reported here was 2.0-mm-long, although other lengths have also been utilized. The transverse confinement was provided by a 3.5-μm-wide ridge waveguide. The active layer consisted of three 8-nm-thick InGaAsP quantum wells with 1% compressive strain separated by 10-nm-thick barriers in the middle of a 0.45-μm-thick optical confinement layer. This material is the same as was used for the tapered amplifiers discussed in the following section, and is described more fully in [4].

This device produced 55-mW/facet output (both ends emitted equally as this device had no coatings) at the operating

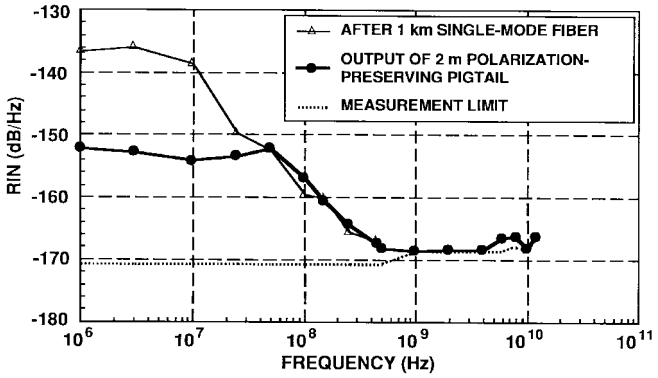

Fig. 2. RIN of FP LO. The RIN at the chip output, and the RIN after 150 m of polarization-preserving fiber, are almost identical to the RIN at the pigtail output.

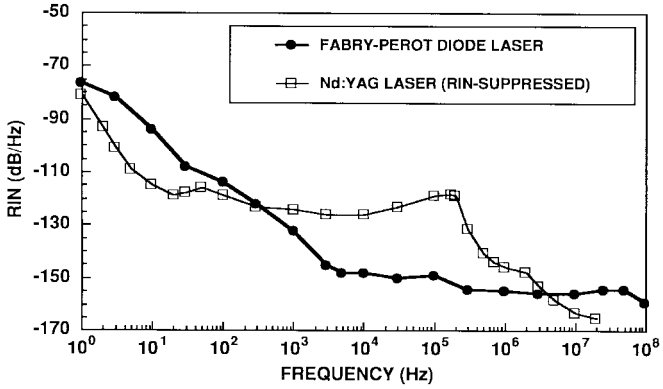

Fig. 3. Low-frequency RIN of semiconductor FP oscillator compared to that of a diode-pumped Nd:YAG laser.

point of 350 mA, of which 32 mW was launched into a polarization-preserving fiber. The threshold was 35 mA.

The RIN-measurement system was calibrated above 10 MHz by measuring the noise level of an Nd:YAG laser beam with the same detector/amplifier/spectrum-analyzer combination as used in the RIN measurement, and then calculating its gain from the known shot-noise power generated by the Nd:YAG laser. This method is the same as we used in [5], but here we have reduced the error to about ± 1 dB at ≤ 500 MHz and ± 2 dB above 500 MHz by repeating the calibration after each measurement. Below 100 kHz, the noise was measured from a detector load resistor in parallel with a high-impedance low-frequency spectrum analyzer, and the RIN could be calculated directly from the dc voltage on the resistor. Between 100 kHz and 10 MHz there was no direct calibration method, but the gain of the detector/amplifier system seemed to be constant, and use of the 10-MHz value was confirmed by agreement at the 100-kHz point with the low-frequency calibrated measurement.

The RIN of the laser output was measured before and after transmission through various lengths of fiber as well as after transmission through the optical links. Fig. 2 shows the RIN-measurement results at the output of the laser pigtail and after transmission through 1-km single-mode fiber. The RIN is <-165 dB/Hz at all frequencies above 500 MHz (the RIN is at the noise floor of our measurement system for most of that range). The RIN before transmission through any fiber, and the RIN after 150 m of polarization-preserving fiber, are almost identical to the RIN from the pigtail, and thus, are not plotted. The relaxation oscillation peak in the RIN is -165 dB/Hz at 8 GHz, barely noticeable above our noise floor. At lower drive currents, the RIN peak is more pronounced; for example, at 68-mA drive, it is -140 dB/Hz at 2 GHz. This type of behavior is expected [6], but the RIN is not generally as low as seen here. The mode spacing on this long laser was 20.6 GHz, so there was a beat frequency present which would be a problem for links including that frequency in their band. Although the RIN of an FP laser is traditionally assumed to be higher than that of a DFB, this is not universally true [7]. In fact, this FP laser's RIN is lower than that of commercially available DFB lasers at microwave frequencies.

The RIN through 150 m of polarization-preserving fiber is virtually identical to the RIN of the laser output before transmission through any fiber. This result applies when the polarization is properly aligned to one of the fiber's axes; if it is misaligned, the noise rises dramatically, as seen in [8]. Transmission through 1 km of single-mode fiber produced an increase in the noise only at frequencies <100 MHz. Thus, even the multimode FP laser can be used over moderate lengths of fiber when the wavelength is near the dispersion zero at 1310 nm.

The one place there is actually an advantage in RIN compared to the Nd:YAG laser is at low frequencies, as seen in Fig. 3. Even though the Nd:YAG laser uses a noise-suppression circuit designed to reduce low-frequency noise and the semiconductor laser does not, the semiconductor laser has lower noise from 300 Hz to 3 MHz. This is an important advantage in microwave links that require low *phase* noise, as the low-frequency noise mixes with an RF signal being transmitted through the link and produces A.M.-noise sidebands on it [9] (which often cause the same system problems as P.M.-noise sidebands).

This low-frequency advantage disappears, however, when the reflections in the link are high enough that optical phase noise (i.e., the laser linewidth) is converted to intensity noise [3]. Fig. 4 shows the low-frequency RIN when the laser light is interfered with a time-delayed version of itself that has been attenuated roughly 50 dB and delayed by a 300-m-long fiber path (equivalent to passing through a pair of -25-dB reflections separated by 150 m of fiber). The Nd:YAG laser through the same link is shown for comparison. It can be seen that the semiconductor laser suffers from somewhat larger noise at low frequencies and that the increased noise extends out to much higher frequencies because of the larger linewidth of the semiconductor laser. For most links, reflections can be suppressed to a degree that this interferometric noise is not a factor; however, in links having high reflections, such as those using a reflective modulator, this effect must be considered.

III. Tapered Semiconductor Optical Amplifier

We have developed a semiconductor optical amplifier with high output power in a single transverse mode by using a tapered structure, as shown in Fig. 5. This structure was first

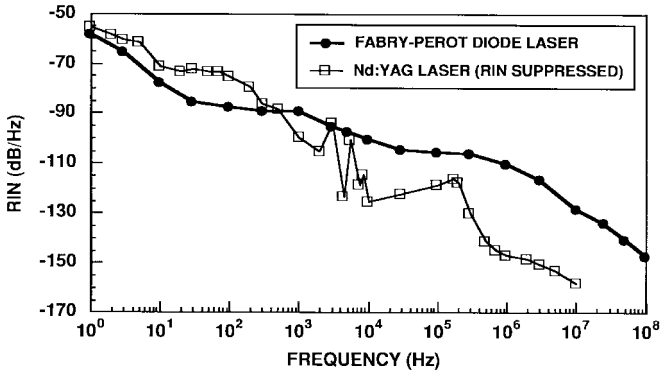

Fig. 4. Increased intensity noise due to optical reflections in a link converting laser linewidth to intensity noise.

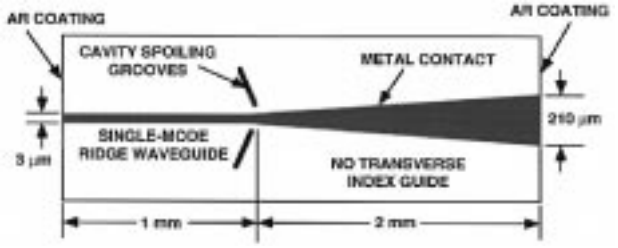

Fig. 5. The tapered amplifier structure. Both facets are antireflection coated.

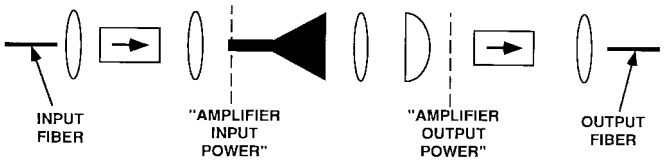

Fig. 6. Tapered amplifier fiber coupling. Amplifier input and output power was measured at the points indicated.

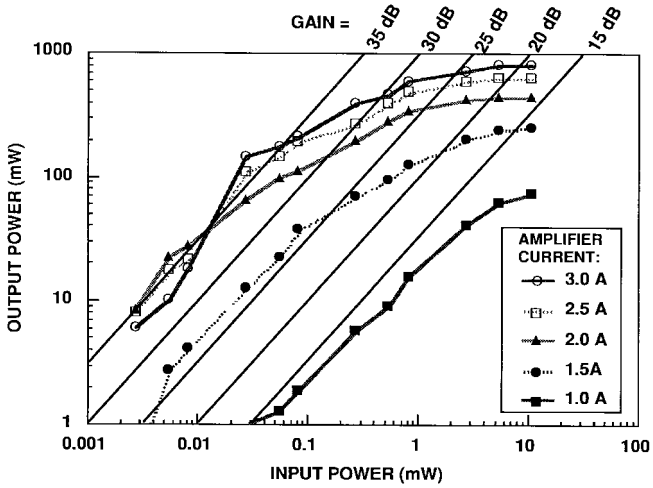

Fig. 7. Tapered semiconductor amplifier input–output power and gain.

built at 980 nm [10]–[12] for pumping EDFA's, and more recently was demonstrated at 1300 nm [5] and 1550 nm [13]. (Some of these references report the structure used as an oscillator, which it is if the input facet is not antireflection coated. However, the noise level of the device as an oscillator currently seems to be too high for use as an analog-link source.) The devices used here are similar to those reported in [5], but here the material has been grown to give a gain peak at 1320 nm, which resulted in higher small-signal gain at the Nd:YAG wavelength of 1319 nm than reported earlier. The active-layer structure is the same as described above for the FP oscillator.

In this device, light is launched into the single-mode waveguide. When it reaches the tapered region, it expands by diffraction; the light is not guided in the transverse direction in the taper. This allows high total power to be generated while keeping the intensity and current density at reasonable values. The drawback is that the output beam is astigmatic and elliptical, requiring anamorphic optics for fiber coupling. Our devices are polarization sensitive, but this is not a problem when used as a CW source for analog links, since polarized light is desired for coupling into most electro-optic modulators.

The fiber coupling setup is shown in Fig. 6. As with any optical amplifier, isolators are required before and after the device for best performance. The input coupling was accomplished with standard spherical diode laser coupling optics. For output coupling, we used a fast (0.55 NA) spherical lens followed by a cylindrical lens to produce a nonastigmatic, approximately circular beam, which was then coupled into a fiber. The amplifier input power was measured in its input waveguide by detecting the photocurrent generated when the amplifier was not biased. The output power was measured in the collimated beam after the first two lenses. When we refer to input and output power and gain, we are referring to power measured at these points. The fiber-coupling efficiency compared the power at these points to the power in the input or output fiber. The highest fiber-to-input waveguide-coupling efficiency we achieved was 60%, and the best output beam-to-fiber efficiency was 43%. Higher output-coupling efficiency should be possible with better lenses and an optimized taper design.

The input–output power characteristics are shown in Fig. 7 for several values of the amplifier drive current. A small-signal gain of 35 dB occurs at 2.0 A, and does not increase at higher currents because of gain clamping due to oscillation in the amplifier. The maximum output power (deep into saturation) is 820 mW at 3.0-A current. With a large input signal, the gain is reduced, and oscillation is damped out so even the 3.0-A drive produces a clean amplified signal. This is shown in Fig. 8, where the single frequency output is obvious.

Several different oscillators could be used with the tapered amplifier to provide a high-power CW source, as diagrammed in Fig. 9. The −3-dB gain bandwidth (as determined from the spontaneous emission with no input) is 21 nm, and there is usable gain over perhaps 50 nm (depending on an individual's definition of usable), so a tunable oscillator can be used. The tapered amplifier can be used with a low-power diode LO, either a DFB laser or an FP laser as described above, or with an Nd:YAG oscillator. While integration of a semiconductor LO and the power amplifier ("MOPA") is possible, the lack of an integratable isolator may cause noise problems due to feedback to the oscillator. The Nd:YAG oscillator may be a practical choice in a broadcast application where many links need to be driven so the oscillator power can be split; we used it because it provided a shot-noise-limited source with which to quantify the noise performance of the amplifier.

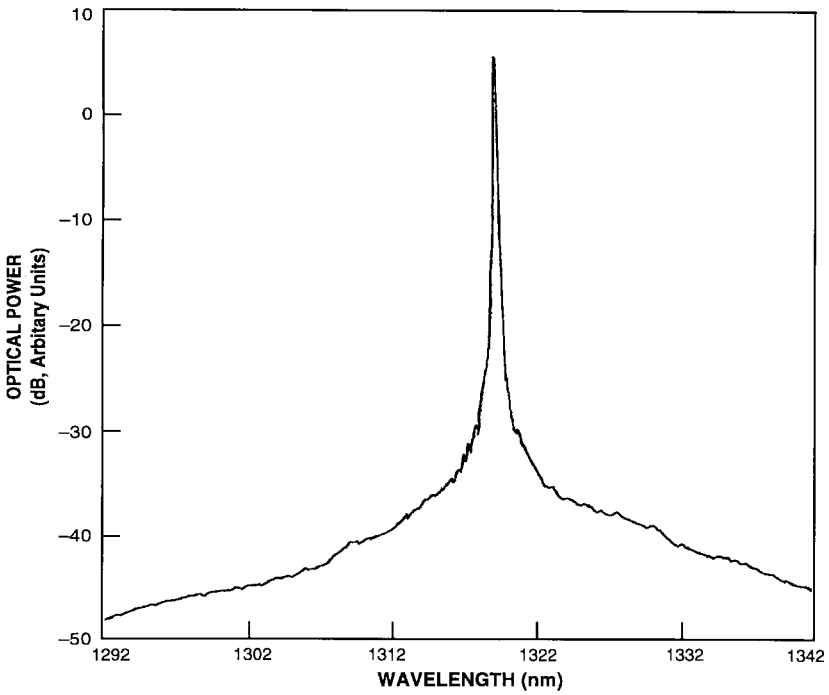

Fig. 8. Amplifier output spectrum at maximum output power of 820 mW (3.0-A amplifier current, 11-mW input from single-frequency Nd:YAG). Taken with 0.1-nm resolution.

TABLE I
SIZE AND "WALL PLUG" EFFICIENCY COMPARISON OF CW SOURCES SUITABLE FOR ANALOG LINKS[1)]

LASER OSCILLATOR OR AMPLIFIER TYPE	VOLUME[2)] (cm^3)	TOTAL ELECTRICAL-TO-OPTICAL EFFICIENCY	EFFICIENCY INCLUDING FIBER COUPLING
1320 nm DIODE-PUMPED ND:YAG	130	0.054	0.043
EDFA, USING SINGLE 500 mW DIODE PUMP	≈100+4	0.06	0.06
TAPERED SEMICONDUCTOR AMPLIFIER	4+4	0.27	0.12

1) Entries do not include volume and efficiency of electrical power supply or cooling components.
2) For amplifiers, size of separate diode oscillator is second number in volume column.

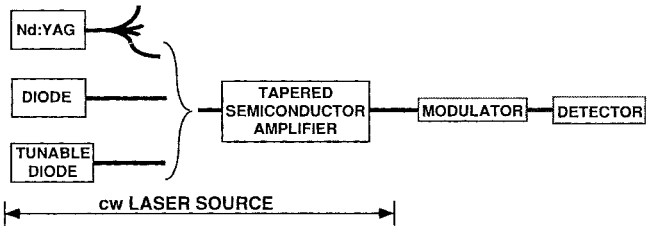

Fig. 9. Possible configurations of CW optical source using the tapered amplifier.

As mentioned in Section I, a significant advantage of this type of device over a DPSSL such as Nd:YAG, or over an EDFA, is its small size and high efficiency. Table I shows a comparison of the size and efficiency of the various devices. The sizes are taken from measurements of the smallest commercially available devices known to us; the EDFA size also involves some assumptions about custom packaging of fiber components. The amplifier efficiencies are the power-added efficiency: light out minus light in, divided by total electrical-power input. High-power EDFA efficiencies range from about 3.5% (DPSSL pump) to 8% (eight multiplexed 1480-nm diode pumps); a midrange value is shown. (This comparison excludes cooling components and the electrical-power supply, which are used by all.)

The RIN spectrum of the tapered amplifier at 1.5- and 2.0-A drive current and 11-mW input is shown in Fig. 10. It is roughly −155 dB/Hz over most of the microwave-frequency range. The RIN does not vary too strongly with drive current in the microwave range, although the RIN below 500 MHz does seem to increase at higher drive current. The RIN at very low frequencies is shown in Fig. 11. In the 1-kHz to 1-MHz range, it is comparable to that of the Nd:YAG oscillator used as input (this single frequency Nd:YAG laser had better low-frequency RIN suppression than the multifrequency Nd:YAG laser used in Figs. 3 and 4). At low frequencies, the output RIN can actually be lower than the input RIN, as seen around 10 kHz, because the amplifier is operated in saturation and the gain for low-frequency intensity fluctuations is much less than

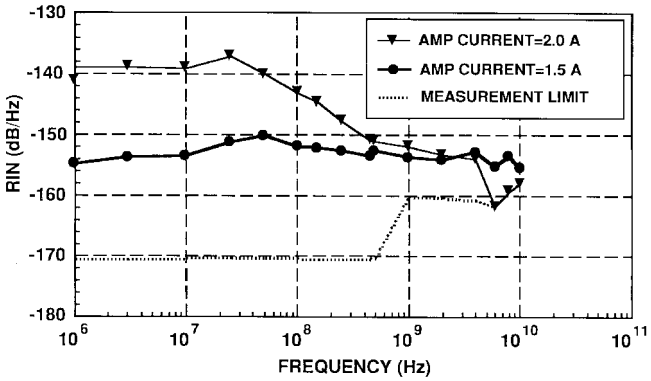

Fig. 10. RIN of the tapered semiconductor amplifier with 11-mW input from a single-frequency Nd:YAG laser.

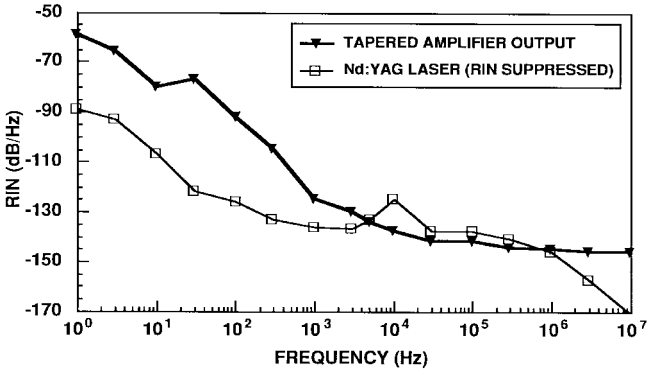

Fig. 11. Low-frequency RIN of tapered semiconductor amplifier output (2.0-A drive, 11-mW Nd:YAG input), compared to RIN of the Nd:YAG LO used as input.

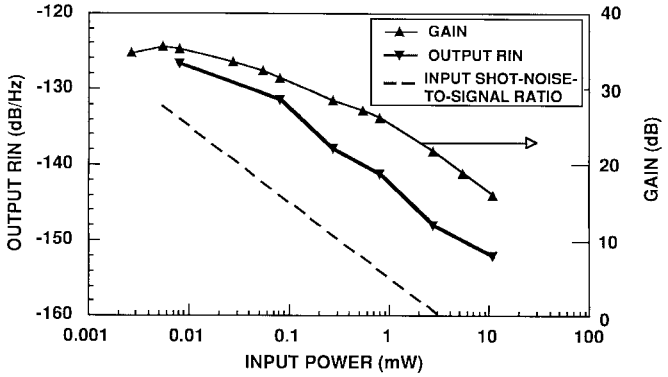

Fig. 12. Tapered semiconductor amplifier RIN at 1 GHz, and gain as functions of optical input power at an amplifier current of 2.0 A. Input shot-noise-to-signal ratio is also shown.

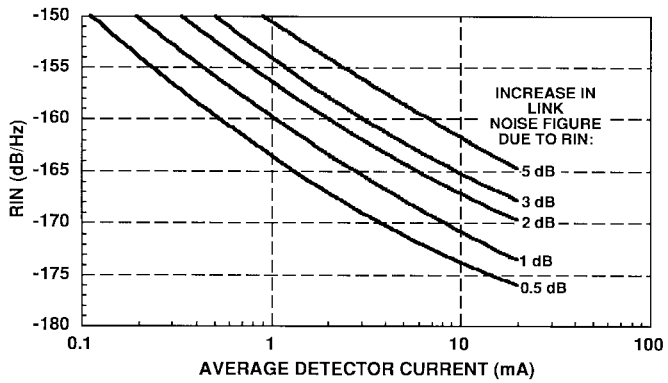

Fig. 13. RIN level causing the indicated increase in link-noise figure relative to a shot-noise-limited link, as a function of average detector current.

the optical gain. Below 1 kHz, the amplifier is contributing significant low-frequency noise of its own.

The RIN varies significantly with input power. As is evident in Fig. 12, the RIN drops as the input power increases. This is not surprising, since larger input power gives larger input signal-to-shot-noise ratio, and the noise figure of the amplifier is approximately constant over much of this range of input power. This amplifier's noise figure is roughly 12 dB. This is higher than is typical for good semiconductor amplifiers, and should be able to be improved with an optimized design.

IV. Link Performance

The sources described above are not ideal in that they are not shot-noise limited. However, links can be designed using them that are very close to the performance of shot-noise-limited links.

A. Limitations Due to RIN, and the Carrier-Suppression Solution

The RIN produces noise at the detector in proportion to the square of the detector current—the same relation to detector current as for the modulated signal. (The average detector current i_{avg} is the dc photocurrent current at the link's operating point, which is the product of the laser power, total optical loss, detector responsivity, and the modulator's transmission at its bias point). The shot noise is linearly dependent on the current, and the receiver thermal noise is independent of the current. Therefore, for a given RIN level, the degradation in link-noise figure and dynamic range is negligible at low detector current, and increases as the current increases. The effect of the RIN at various photocurrent levels can be determined by calculating the electrical-noise figure of a link with no RIN present, then calculating how much worse the noise figure is with the RIN present. This is done in Fig. 13, which shows that the detector current must be restricted to a few milliampere or less to avoid significant degradation in the link-noise figure at the RIN levels of our semiconductor laser sources.

For multioctave-bandwidth links, known modulator types must be biased near their 50% transmission point to minimize second-order distortion, and the restriction on detector current above results in relatively poor performance with even a moderate RIN (externally modulated analog-link performance improves as the optical power increases [14], [15]). High dynamic range can still be achieved in this case by using a broad-band linearized modulator [16], although noise figure will still suffer. If one can tolerate a more complex system, the RIN can be canceled by using a balanced receiver [17] or by using optical feedforward error correction [18].

For suboctave-bandwidth links, there is a simple way to recover performance nearly equal to that of links powered by shot-noise-limited sources: the optical carrier can be suppressed by biasing a Mach–Zehnder (MZ) interferometric modulator toward its minimum transmission point [19]–[21]. This can be understood by examining Fig. 14. The bias point

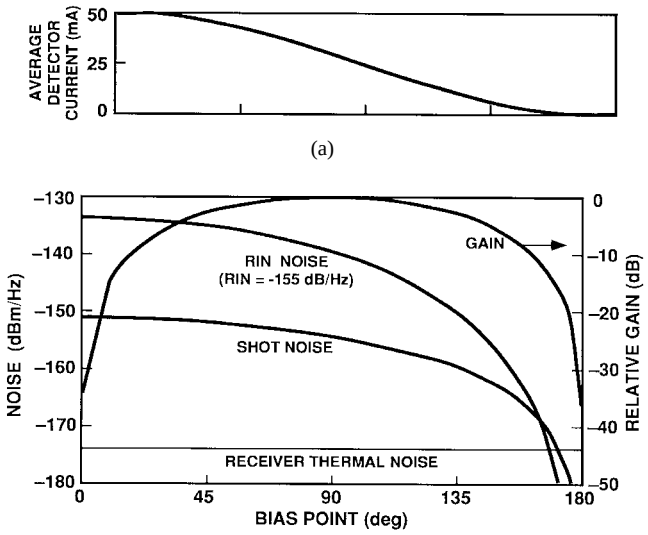

Fig. 14. Effect of varying the bias point of a MZ interferometric modulator, calculated for a full-on detector current of 50 mA. (a) Average detector current, (b) output noise sources, and link electrical gain (gain shown relative to the gain at 90° bias).

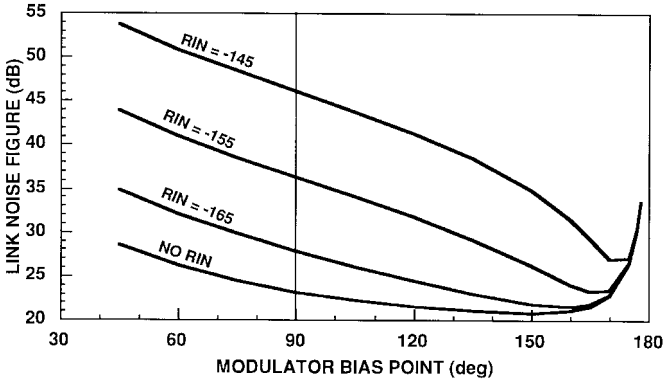

Fig. 15. Effect of modulator bias point on link electrical-noise figure, calculated for a full-on (0° bias) detector current of 40 mA, modulator V_π of 5 V, and receiver noise figure of 0 dB.

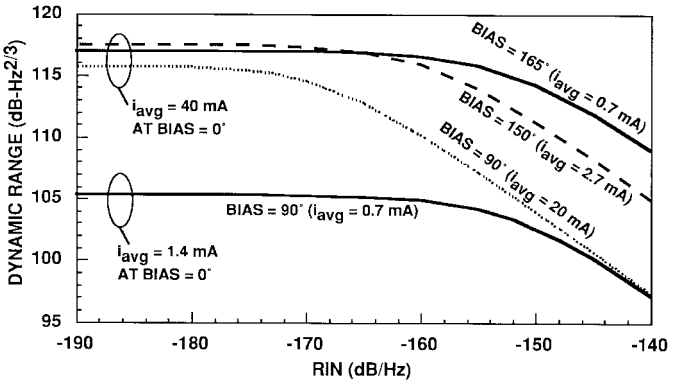

Fig. 16. Third-order intermodulation-free dynamic range as a function of the RIN for various modulator bias points. Curves are also labeled with the average detector current ($i_{\rm avg}$). Two full-on (0° bias) detector currents are shown.

for 50% transmission is 90°. This gives the maximum link electrical gain. As the bias point θ is moved toward 180°, the optical transmission falls rapidly (as $1+\cos\theta$). The shot noise falls linearly with the optical transmission, and the RIN noise falls as the square of the optical transmission. The link gain, however, falls much more slowly (as $\sin^2\theta$). The net result is that the output electrical signal-to-noise ratio rises as the bias point moves toward 180°, until the gain is so small that receiver thermal noise dominates. For shot-noise-limited links, the signal-to-noise ratio improvement relative to the value at 90° is limited to 3 dB; for RIN-dominated links, there is no limit to the improvement (until receiver thermal noise is reached).

There are other ways to suppress the carrier, such as optical filtering before the detector, but these offer no performance advantage and are harder to implement [22]. The technique of suppressing the optical carrier by biasing a modulator toward its off state can be used with many different types of modulator, including linearized modulators [16], [23], [24], as well as more standard designs.

The improvement in a link-noise figure with suppressed-carrier bias is shown for several RIN levels in Fig. 15, for a link using an MZ modulator with a V_π of 5 V, a detector current of 40 mA at 0° bias, and a receiver noise figure of 0 dB. For a RIN of -155 dB/Hz, performance near that of the shot-noise-limited case is obtainable. The third-order intermodulation-free dynamic range is to 0.67 $(\mathrm{IIP3}-\mathrm{NF}+174)$, where IIP3 is the modulator's input third-order intercept point in decibels with reference to a power level of one milliwatt (dBm) and NF is the link-noise figure in decibels. Since IIP3 does not vary with bias point, the dynamic range increases as the noise figure decreases.

The above discussion of carrier suppression, using Figs. 14 and 15, took the viewpoint that the laser power and RIN were fixed. The link performance with the RIN present could be recovered to the link performance available with the same laser power but no RIN (shot-noise-limited) by carrier suppression.

An alternative viewpoint to take is to look at the detector current as fixed (for example, by picking a detector current off Fig. 13 for a given RIN level and noise-figure degradation). Then the input laser power can be increased and the MZ's bias point set at a lower transmission value to keep the detector current constant. This can be seen in Fig. 16 by comparing the two curves with $i_{\rm avg}=0.7$ mA. The lower curve corresponds to using the 90° bias point with a low laser power ($i_{\rm avg}=1.4$ mA at 0° bias), and the upper curve corresponds to a suppressed carrier bias point of 165°, but with high laser power ($i_{\rm avg}=40$ mA at 0° bias). The dynamic range is 12 dB larger for the upper curve at all RIN levels. This is the viewpoint of [20], which regards carrier suppression as a dynamic range-improvement technique.

B. Links Using the Tapered Amplifier Source

The first experiment we performed was a direct comparison between a link using the Nd:YAG laser and a link using the source consisting of the attenuated Nd:YAG output driving the tapered amplifier. In both cases, the link configuration was the same: the laser source, 150-m polarization-preserving fiber, a standard MZ modulator, 150-m single-mode fiber, and an InGaAs p-i-n detector. The tapered amplifier output was

TABLE II
MICROWAVE LINK PERFORMANCE COMPARISON

LASER TYPE	TEST FREQUENCY (GHz)	LASER POWER (mW)	MODULATOR TYPE	AVERAGE DETECTOR CURRENT (mA)	THIRD-ORDER INTERMODULATION-FREE DYNAMIC RANGE (dB-Hz$^{2/3}$)
ND:YAG (REF. [17])	17	?	MACH-ZEHNDER INTERFEROMETER	1.5	115
TAPERED AMPLIFIER	2	240	MACH-ZEHNDER INTERFEROMETER	4.0	113
TAPERED AMPLIFIER	6	240	MACH-ZEHNDER INTERFEROMETER	4.0	111
TAPERED AMPLIFIER	10	240	MACH-ZEHNDER INTERFEROMETER	4.0	111
FP OSCILLATOR	2	32	LINEARIZED	0.12	111

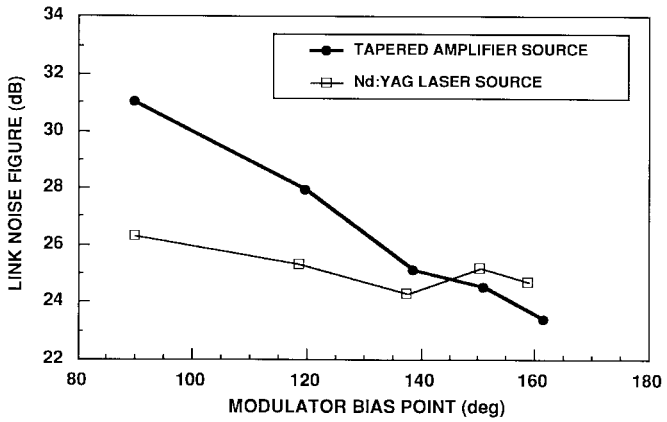

Fig. 17. Noise figure of an analog link at 450 MHz using the tapered semiconductor amplifier CW source, compared to the same link using a Nd:YAG laser source. Both sources provided about 100-mW input to the modulator.

attenuated to match the 100-mW power level available from the Nd:YAG laser. The link-noise figure was measured at 450 MHz, at various modulator bias points. The results are plotted in Fig. 17. The results are just as expected from the theoretical considerations discussed above. The noise figure with the tapered amplifier is higher at the 90° bias point, where the detector current is about 6 mA. Both links show improved noise figure as the bias point moves toward 180°, with the greater improvement occurring in the tapered amplifier link with its higher RIN. At 150°–160° bias point the noise figure is identical for both laser sources, within the experimental error. This is consistent with a tapered amplifier RIN of ≤ -155 dB/Hz.

To demonstrate the performance potential of links at microwave frequencies powered by the tapered amplifier, we measured the dynamic range of a link consisting of the Nd:YAG oscillator/tapered-amplifier source, a few meters of polarization-preserving fiber, a 7-GHz-bandwidth MZ modulator, a few meters of single-mode fiber, and an InGaAs p-i-n detector. The power in the input fiber was 240 mW, which was as high as we were able to obtain at the time the experiment was performed. We biased the modulator at $\approx$155°, which reduced the dc detector current to 4.0 mA. This was the maximum current this detector could handle, independent of RIN considerations. We measured the noise figure and dynamic range at 2, 6, and 10 GHz. Our noise figures of 30–42 dB were high because of the high V_π of the modulator used in the experiment. The dynamic range results are shown in Table II, along with the best dynamic range result reported in the literature for a microwave link using a standard MZ modulator. It is clear that the tapered amplifier powered link is competitive in dynamic range performance.

C. Link Using FP Diode LO

In order to demonstrate how use of a linearized modulator can provide adequate link dynamic range with very low received power, we made a link consisting of the semiconductor FP LO described above, a series MZ linearized modulator [23], 1-km single-mode fiber, and the usual InGaAs p-i-n detector. The input fiber power was 32 mW, and the optical loss of the link was 13 dB, resulting in an average detector current of only 0.12 mA at the modulator's operating bias point (about 12% transmission). The dynamic range was still 111 dB/Hz$^{2/3}$, comparable to links using high-power Nd:YAG lasers and standard modulators. Although this was a suboctave linearized modulator, the same dynamic range could be achieved in a broad-band link if a broad-band linearized modulator were used.

V. CONCLUSION

We have demonstrated a semiconductor optical amplifier with high output power (820 mW) and low RIN (≈ -155 dB/Hz at microwave frequencies). We have also demonstrated an FP semiconductor LO with very low RIN (< -165 dB/Hz above 500 MHz). These semiconductor sources offer advantages over the usual DPSSL sources in the areas of size, efficiency, and wavelength flexibility. They also can be quieter at very low frequencies (<1 MHz), potentially leading to links with lower RF phase noise. We have theoretically shown how the carrier-suppression bias technique can be used in suboctave-bandwidth links with sources having these RIN levels to achieve performance comparable to that of links with shot-noise-limited sources. We have also constructed some

experimental links which prove the performance capability of links using these CW semiconductor sources.

The semiconductor sources still have RIN levels too high to support very high performance multioctave links with standard modulators. However, by using a linearized modulator and low received power, they can perform adequately even in this application.

Finally, it should be noted that the tapered amplifiers used in this paper have not yet been optimized for minimum noise figure, and some improvement should be possible.

ACKNOWLEDGMENT

The author would like to acknowledge K. G. Ray for fabrication of some of the modulators used in this paper, and L. M. Johnson for helpful discussions.

REFERENCES

[1] D. R. McElroy, W. C. Cummings, and D. P. Kolba, "Lightweight adaptive antennas for EHF payloads," in *IEEE MILCOM'92 Tech. Dig.*, San Diego, CA, Oct. 11–14, 1992, pp. 924–928.

[2] H. Zmuda and E. N. Toughlian, Eds., *Photonic Aspects of Modern Radar*. Norwood, MA: Artech House, 1994.

[3] J. L. Gimlett and N. K. Cheung, "Effects of phase-to-intensity noise conversion by multiple reflections on gigabit-per-second DFB laser transmission systems," *J. Lightwave Technol.*, vol. 7, pp. 888–895, June 1989.

[4] S. H. Groves, J. P. Donnelly, J. N. Walpole, J. D. Woodhouse, L. J. Missaggia, R. J. Bailey, and A. Napoleone, "Strained-layer InGaAsP diode lasers with tapered gain region for operation at $\lambda = 1.3\,\mu$m," *IEEE Photon. Technol. Lett.*, vol. 6, pp. 1286–1288, Nov. 1994.

[5] J. P. Donnelly, J. N. Walpole, G. E. Betts, S. H. Groves, J. D. Woodhouse, F. J. O'Donnell, L. J. Missaggia, R. J. Bailey, and A. Napoleone, "High-Power 1.3-μm InGaAsP-InP amplifiers with tapered gain regions," *IEEE Photon. Technol. Lett.*, vol. 8, pp. 1450–1452, Nov. 1996.

[6] K. Y. Lau, N. Bar-Chaim, I. Ury, C. Harder, and A. Yariv, "Direct amplitude modulation of short-cavity GaAs lasers up to X-band frequencies," *Appl. Phys. Lett.*, vol. 43, pp. 1–3, July 1983.

[7] H. V. Roussell, R. Helkey, G. E. Betts, and C. H. Cox III, "Effect of optical feedback on high dynamic range Fabry–Perot laser optical links," *IEEE Photon. Technol. Lett.*, vol. 9, pp. 106–108, Jan. 1997.

[8] C. H. Bulmer, R. P. Moeller, and W. K. Burns, "Effect of phase noise in linear modulator systems," *Appl. Opt.*, vol. 31, pp. 6437–6440, Oct. 1992.

[9] K. Y. Lau and H. Blauvelt, "Effect of low-frequency intensity noise on high-frequency direct modulation of semiconductor injection lasers," *Appl. Phys. Lett.*, vol. 52, pp. 694–696, Feb. 1988.

[10] J. N. Walpole, E. S. Kintzer, S. R. Chinn, C. A. Wang, and L. J. Missagia, "High-power, strained-layer InGaAs/AlGaAs tapered traveling wave amplifier," *Appl. Phys. Lett.*, vol. 61, pp. 740–742, Aug. 1992.

[11] D. F. Welch *et al.*, "1.1 W diffraction-limited operation of monolithically integrated flared amplifier master oscillator power amplifier," *Electron. Lett.*, vol. 28, pp. 2011–2013, Oct. 1992.

[12] P. S. Yeh, I. F. Wu, S. Jiang, and M. Dagenais, "High-power, high-gain monolithically integrated preamplifier/power amplifier," *Electron. Lett.*, vol. 29, pp. 1981–1982, Oct. 1993.

[13] J. P. Donnelly, J. N. Walpole, S. H. Groves, R. J. Bailey, L. J. Missagia, and A. Napoleone, "High-power 1.5-m InGaAsP/InP lasers with a tapered gain region" to be presented at the *IEEE Lasers and Electro-Optics Soc. 1997 Annu. Meeting,"* San Francisco, CA, Nov. 10–13, 1997.

[14] G. E. Betts, L. M. Johnson, and C. H. Cox III, "Optimization of externally modulated analog optical links,"*Proc. SPIE–Int. Soc. Opt. Eng.*, vol. 1562, pp. 281–302, July 1991.

[15] C. H. Cox III, G. E. Betts, and L. M. Johnson, "An analytic and experimental comparison of direct and external modulation in analog fiber-optic links," *IEEE Trans. Microwave Theory Tech.*, vol. 38, pp. 501–509, May 1990.

[16] W. B. Bridges and J. H. Schaffner, "Distortion in linearized electrooptic modulators," *IEEE Trans. Microwave Theory Tech.*, vol. 43, pp. 2184–2197, Sept. 1995.

[17] E. Ackerman, S. Wanuga, J. MacDonald, and J. Prince, "Balanced receiver external modulation fiber-optic link architecture with reduced noise figure," in *IEEE MTT-S Int. Microwave Symp. Dig.*, Atlanta, GA, June 14–18, 1993, pp. 723–726.

[18] R. J. Plastow, "80-channel AM-VSB CATV transmitters utilizing external modulation and feedforward error correction," in *1992 IEEE LEOS Summer Topical Meeting on Broad-Band Analog and Digital Optoelectronics Tech. Dig.*, Santa Barbara, CA, July 1992, pp. 10–11.

[19] G. E. Betts and F. J. O'Donnell, "Improvements in passive, low-noise-figure optical links," presented at the *Photonics Syst. Antenna Applicat. III*, Monterrey, CA, Jan. 20–22, 1993.

[20] M. L. Farwell, W. S. C. Chang, and D. R. Huber, "Increased linear dynamic range by low biasing the Mach-Zehnder modulator," *IEEE Photon. Technol. Lett.*, vol. 5, pp. 779–782, July 1993.

[21] E. I. Ackerman, S. Wanuga, D. Kasemset, A. S. Daryoush, and N. R. Samant, "Maximum dynamic range operation of a microwave external modulation fiber optic link," *IEEE Trans. Microwave Theory Tech.*, vol. 41, pp. 1299–1306, Aug. 1993.

[22] M. J. LaGasse, W. Charczenko, M. C. Hamilton, and S. Thaniyavarn, "Optical carrier filtering for high dynamic range fiber optic links," *Electron. Lett.*, vol. 30, pp. 2157–2158, Dec. 1994.

[23] G. E. Betts, "A linearized modulator for sub-octave-bandpass optical analog links," *IEEE Trans. Microwave Theory Tech.*, vol. 42, pp. 2642–2649, Dec. 1994.

[24] C. K. Sun, S. A. Pappert, R. B. Welstand, J. T. Zhu, P. K. L. Yu, Y. Z. Liu, and J. M. Chen, "High spurious-free dynamic range fiber link using a semiconductor electroabsorption modulator," *Electron. Lett.*, vol. 31, pp. 902–903, May 1995.

Gary E. Betts (S'84–M'84) was born in Seattle, WA, on May 14, 1954. He received the B.S. degree in physics from Haverford College, Haverford, PA, in 1976, the M.S. degree in physics and the Ph.D. degree in applied physics from the University of California at San Diego, in 1980 and 1985, respectively.

From 1976 to 1978, he worked in integrated optics, primarily on the design of geodesic lenses, at the Westinghouse Electric Corporation, Baltimore, MD. Since 1985, he has been a Staff Member at the Massachusetts Institute of Technology (MIT) Lincoln Laboratory, Lexington, working primarily on lithium–niobate integrated-optical modulators and analog fiber optic links. His work at MIT has included microwave-frequency modulators, low-frequency modulators with very high sensitivity, linearized modulators, investigation of optical damage and other drift phenomena in lithium niobate, and most recently, work on high-powered semiconductor optical amplifiers.

Dr. Betts is a member of the Optical Society of America and the IEEE Lasers and Electro-Optics Society.

J. P. Donnelly (S'60–M'63–SM'88–F'90), photograph and biography not available at the time of publication.

J. N. Walpole (S'60–M'61–SM'94–F'96), photograph and biography not available at the time of publication.

S. H. Groves, photograph and biography not available at the time of publication.

F. J. O'Donnell, photograph and biography not available at the time of publication.

L. J. Missaggia, photograph and biography not available at the time of publication.

R. J. Bailey, photograph and biography not available at the time of publication.

A. Napoleone, photograph and biography not available at the time of publication.